Title

Split Reflections from Broken Mirrors: Symmetry Breaking in the Making of Materials Microstructures

Author

Dahmen, U.

Publication Date

1992-10-01

LBL-33474
UC-404

Lawrence Berkeley Laboratory
UNIVERSITY OF CALIFORNIA

Materials Sciences Division

National Center for Electron Microscopy

Presented at the Microstructures of Materials Conference,
Berkeley, CA, October 22–23, 1992, and to
be published in the Proceedings

Split Reflections from Broken Mirrors: Symmetry Breaking in the Making of Materials Microstructures

U. Dahmen

October 1992

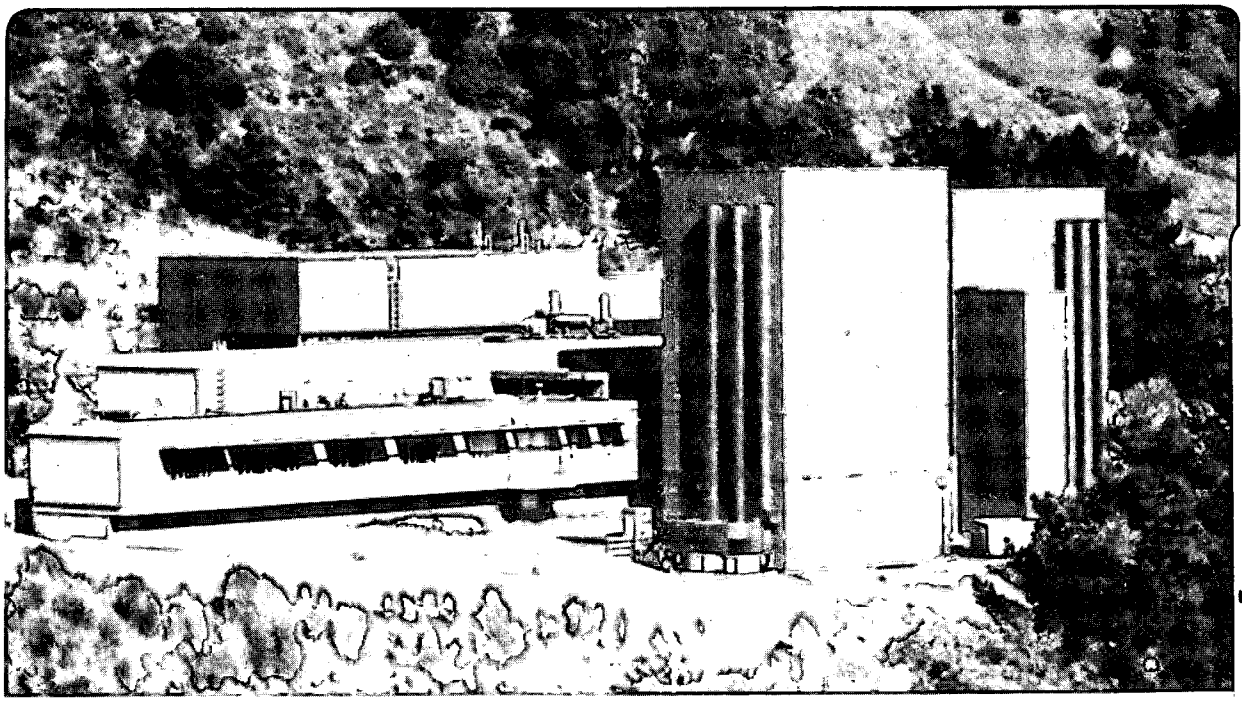

Prepared for the U.S. Department of Energy under Contract Number DE-AC03-76SF00098

DISCLAIMER

LBL-33474

Split Reflections from Broken Mirrors: Symmetry Breaking in the Making of Materials Microstructures

U. Dahmen

Materials Science Division
National Center for Electron Microscopy
Lawrence Berkeley Laboratory
University of California, Berkeley, CA 94720

Proc. of the Microstructures of Materials Conf.
10/22-10/23/92, Berkeley, CA

This work was supported in part by the Director, Office of Energy Research, Office of Basic Energy Sciences, Materials Science Division of the U.S. Department of Energy under Contract No. DE-AC03-76SF00098.

Split Reflections from Broken Mirrors: Symmetry-Breaking in the Making of Materials Microstructures

Ulrich Dahmen
National Center for Electron Microscopy
Materials Sciences Division
Lawrence Berkeley Laboratory
Berkeley, California 94720

Abstract

The symmetry underlying the development of microstructure in materials is a global property with great practical uses in the design and analysis of precipitate distributions and morphologies, orientation relationships between crystals, properties of interfaces and textures and topographies of microstructures.

I. INTRODUCTION

In the study of microstructure, transmission electron microscopy plays a unique role because it provides access to features in the size range of about 1μm to atomic dimensions. This is the range where many of the important properties of a material are controlled. Tensile strength, ductility, resistance to fatigue, wear or corrosion, coercivity, high temperature deformation behavior are but a few of the many materials properties that are directly linked to microstructure at the sub-micron level. Electron microscopy has played a key role in defining this link and is becoming an increasingly important tool in the characterization and design of materials.

However, in the steady development of microscopy towards higher resolution, some of the more global aspects of microstructure, well-known to early mineralogists and crystallographers, have been neglected. By focusing on a small section of one interface of one precipitate in one grain of a material, its connection with other interfaces, other precipitates and other grains is often lost. This loss of perspective on the connection with the whole microstructure is a consequence of the microscopists quest for spatial resolution.

Crystal symmetry provides an abundance of information that can be used to facilitate and improve the TEM analysis of two-phase structures. The present contribution is a reminder of the symmetries underlying microstructural development and the possibilities for using global or broken symmetries in the TEM analysis and the design of microstructures in crystalline solids.

II. RESULTS AND DISCUSSION

A. Point Symmetry in Orientation Relationships

Orientation relationships between crystals, across grain or interphase boundaries, are an important defining characteristic of a microstructure. Most orientation relationships are derived from phase transformations and as a result are non-random, and often maintain a high degree of common symmetry.

Consider the common case of a precipitate of cubic crystal structure (e.g. bcc, fcc, diamond, sphalerite, simple cubic) growing inside matrix that also has cubic crystal structure. The shape and distribution of the precipitates and through it the properties of this two-phase material will depend critically on the orientation relationship that is adopted. If the cube axes are aligned, the orientation relationship is known as parallel cube or cube-cube. This is the simplest and most highly symmetric case. Fourfold, threefold or twofold symmetry axes as well as mirror planes of the two crystals are aligned and therefore common to matrix and precipitate. Examples of this case are the cuboidal precipitates in high temperature superalloys or $M_{23}C_6$ precipitates austenitic stainless steel.

Structural phase transformations can be described by a transformation strain that distorts the parent into the product lattice. The transformation strain depends on the lattice correspondence, i.e. a unit cell of the parent which, by distortion, becomes a unit cell of the product. Often these strains are simple and of high symmetry [1]. For example the Bain correspondence between fcc and bcc lattices requires a distortion along the common cube axis and a different strain in the plane normal to this axis, giving it cylindrical symmetry (Curie group ∞/mm). However, fcc-bcc transformations usually lead to much lower composite symmetry than that of the Bain correspondence. The reason for this symmetry-breaking is the fact that the strain energy of the assembly can be lowered if in addition to the Bain strain the transformation product lattice undergoes a rotation to produce a strain-free (invariant) line or plane at the interface [2]. This rotation determines the orientation relationship, and as it is controlled entirely by the magnitude of the strains, it follows that orientation relationships are often irrational.

B. Symmetry Breaking and Spot Splitting

An example of a composite diffraction pattern showing an irrational orientation relationship between an fcc matrix and a bcc precipitate is seen in Fig. 1. The traces of mirror planes in both phases are outlined: vertical and horizontal for the <110> zone axis of the fcc matrix and in a threefold star, at 120° to one another for the <111> zone axis of the bcc precipitate whose {112} spots are marked by black arrows. It is clear that the relative rotation between the lattices destroys any common mirror or rotation symmetries, leading to low composite symmetry. However, from the separation between corresponding diffraction spots (spot splitting, indicated by white arrows) it can also be seen that the same rotation

produces an invariant plane strain, characterized by a single direction of spot splitting.

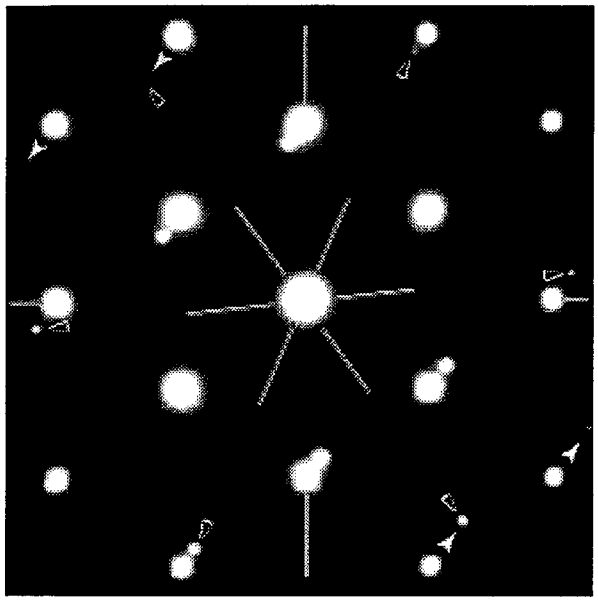

Figure 1: Composite diffraction pattern of bcc precipitate in fcc matrix related by an invariant line strain, showing misalignment of mirror planes (white lines) and uniform direction of spot splitting (white arrows).

An invariant plane strain will always lead to a characteristic diffraction pattern with a single direction of spot splitting [3]. This illustrated schematically in figure 2. The orientation relationship of high symmetry with common mirror planes in a) is reduced to one of low symmetry in b) by adding a small rotation. As a result of this lattice rotation,

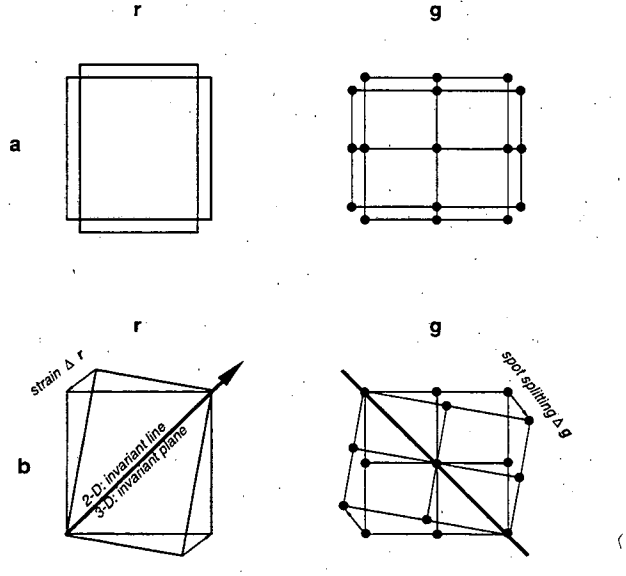

Figure 2: Schematic illustration of transformation from a square to a rectangular lattice in real space **r** (left column) and reciprocal space **g** (right column). In a), mirror planes are aligned and the orientation relationship is of high symmetry. In b), a relative lattice rotation has been added to produce an invariant line or plane. The effect of this lattice rotation is a single direction of spot splitting in the diffraction pattern.

there is now a line or plane of perfect matching in the bicrystal. A precipitate lying along this line or on this plane will have low strain or interface energy. The symmetry-breaking is thus due to the minimization of elastic energy [4].

From figure 2 it is also apparent that the direction of spot splitting in the diffraction pattern will be perpendicular to the invariant line or plane of the precipitate. The origin of this effect is apparent from geometry of the transformation.

C. The Moiré Equivalent

An alternative illustration of this effect with the aid of the moiré effect is shown in figure 3. The upper part of this schematic shows a mixed moiré pattern, i.e. two lattices slightly mismatched in both orientation and spacing, and the corresponding diffraction vectors $\mathbf{g}_1$, $\mathbf{g}_2$ and $\Delta\mathbf{g}$. The moiré fringes are normal to $\Delta\mathbf{g}$ and their spacing is inversely proportional to $|\Delta\mathbf{g}|$. If one of the two lattices is shrunk to be enclosed in the other, as shown in the lower part of the schematic, then it represents the case of a misfitting precipitate in a matrix. The misfit does not change along the moiré fringes but alternates between good and bad match perpendicular to the fringes. Hence the interfaces between precipitate and matrix will match well if it lies along the moiré fringes, i.e. perpendicular to the direction $\Delta\mathbf{g}$ of spot splitting.

It is further interesting to note that a small rotation α in the orientation relationship will lead to a large rotation θ of the moiré pattern and hence also in the optimum plane or line of contact. Measurements of orientation relationships must therefore be made with greater accuracy than measurements of habit planes if the two are to be related by theoretical modelling.

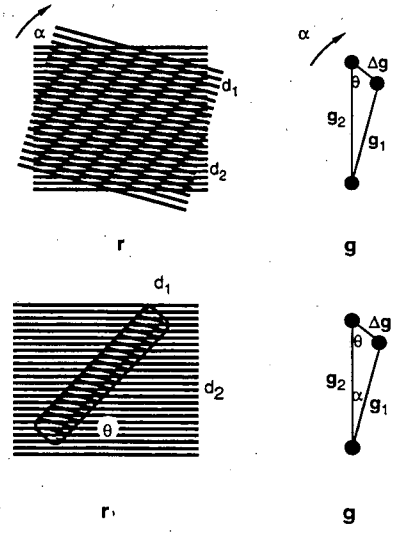

Figure 3: Schematic illustration of the relationship between moiré patterns and the optimum orientation of a misfitting precipitate and its direction of spot splitting in the diffraction pattern.

Notice that in the examples of figure 2 and 3 an anticlockwise rotation would lead to a mirror-related invariant line or -plane strain, i.e. a different variant of the same orientation relationship. Thus, as a result of symmetry-breaking the number of equivalent orientations or variants increases. Generally, the lower the composite symmetry, the more orientation variants are possible.

D. Symmetry Relations Between Variants

It has been pointed out by a number of authors (e.g. 3,5,6) that different variants of a precipitate in a given matrix are related to each other by symmetry elements of the matrix. This is illustrated schematically in figure 4 where the variant-generating symmetry operation is either a 90° rotation or a reflection across the diagonal mirror plane. Only those symmetry elements of the matrix that are not shared by the precipitate generate new variants. The remaining symmetry elements of the matrix, those that *are* shared by the precipitate, define the point group of the orientation relationship, i.e. the bicrystal symmetry. Thus the number of orientation variants is the index of the point group of the bicrystal in the point group of the matrix, i.e. the ratio of the number of symmetry elements in the two groups.

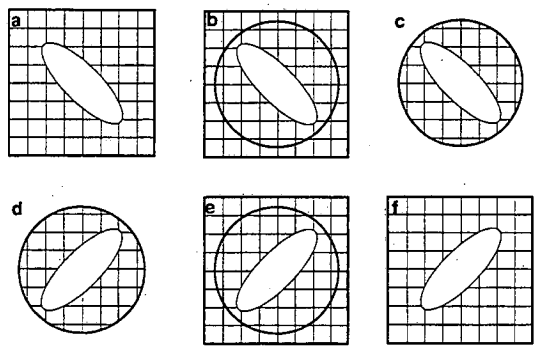

Fig. 4 Schematic illustration of variant-generating symmetry operation in a cubic matrix

It has been shown [7] that according to Curie's principle the equilibrium shape of a precipitate in a matrix must have at least the symmetry of the orientation relationship [8]. For a cube-cube orientation relationship this permits precipitates of cubic and higher symmetry, e.g. cubes, octahedra, tetrahedra or spheres. An orientation relationship with low symmetry will lead to many variants of low-symmetry-shaped precipitates and vice versa. In Fig. 5 this is illustrated with a micrograph showing a field of Cr precipitates in a Cu matrix. 24 different variants of the Cr laths can be counted, and their faceted low-symmetry shape, corresponding to the orientation relationship shown in Fig. 1, is apparent from those particles that are seen nearly end-on.

Each variant-generating symmetry operation may be considered a crystal tilt in a trace analysis, and it has been shown that by measuring angles between symmetry-related variants it is thus possible to determine the direction of needle- or lath-shaped precipitates from a single micrograph [9]. The Miller indices of a needle-shaped precipitate is found from the following relations by measuring two angles α and β between variants related to each other by reflection across a {100} mirror plane of the matrix (see schematic in figure 6):

$$h^2/l^2 = (1-\cos\alpha)/(1+\cos\alpha) \quad (1)$$

$$h^2/k^2 = (1-\cos\beta)/(1+\cos\beta), \quad (2)$$

where $\alpha, \beta < 90°$.

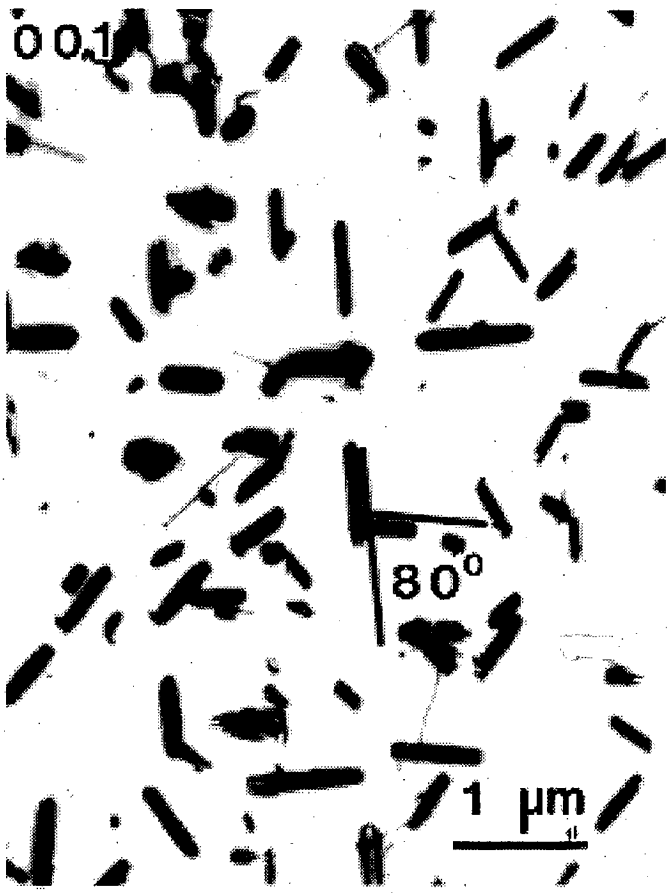

Figure 5: Distribution of <761> needle precipitates in Cu-0.3%Cr alloy, quenched and aged 18h at 700°C, seen in <001> projection. One intervariant angle , $\alpha = 80°$ is indicated.

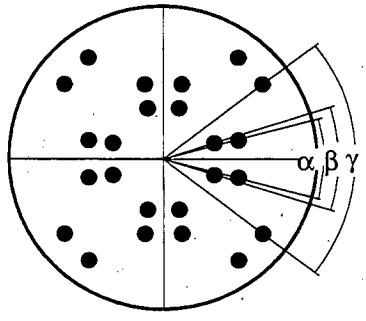

Figure 6: <001> stereogram of needle axes with general direction of type <hkl> showing intervariant angles.

The same principle can be used to improve the accuracy of conventional trace analysis: by measuring angles between

variants of precipitates the rotation between image and diffraction pattern is eliminated as a source of error [10].

A simpler precipitate distribution, of the type <hhl> is shown in figure 7. Schematically, the projected shapes of all 12 orientation variants of an <hhl> needle precipitate in a cubic matrix are gathered around a common point at the right. Notice how the variants near the perimeter of the stereogram have more elongated shapes in the schematic projection. In a crystalline matrix, all orientation variants are usually distributed at random locations, as shown in the frame below.

One may now imagine the precipitates growing to impingement, consuming the matrix crystal entirely. For a uniform distribution and equal growth rates, this would eventually lead to the hexagonal grain structure illustrated in the lower frame. Each grain corresponds to one of the 12 orientation variants. Where two identical variants impinge they form a single grain. All others form a grain boundary with a characteristic misorientation. The resulting polycrystal is highly textured because it originated in a single crystal. Even though, locally grain boundaries have high angle misorientations, globally, the microstructure maintains the cubic symmetry of the parent phase.

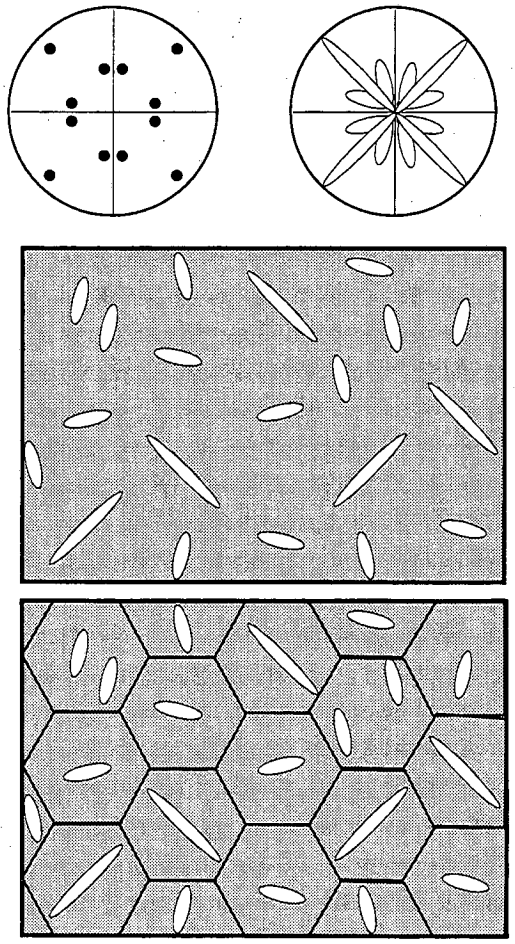

Figure 7: Illustration of <hhl> precipitate variants in a cubic matrix, shown stereographically and schematically in <001> projection. Growth to impingement will eliminate the matrix crystal and lead to a textured polycrystal.

Many microstructures may be thought of as originating in a similar manner. For example, during martensitic transformations, a single matrix grain of a cubic crystal may give rise to as many as 48 orientation variants of the martensitic phase.

E. Mazed Multicrystal Microstructures

The same principle can be applied to the synthesis of highly textured "mazed multicrystal" microstructures by thin film deposition [11]. For example, if a thin film of one material is deposited on a single crystal of another material, then a textured polycrystal of the type described above will result. The number and type of orientation variants, and hence the degree of texture depend on the heteroepitaxial orientation relationship preferred by the system. Al on (001) Si substrates, under well-defined conditions, will form only two orientation variants [12]. The honeycomb network shown in the bottom frame of figure 7 will thus be occupied at random by only two grain orientations. This results in a "mazed bicrystal" structure shown in figure 8, left side. Note that with only two grain orientations there is only one type of grain boundary and no triple junctions.

On a {111} Si substrate, Al forms three orientation variants, leading to a "mazed tricrystal" structure illustrated schematically in figure 8, right side. The three grain orientations are indicated by three different shadings. In this microstructure, triple junctions are possible, but all boundaries are of the same 120° misorientation. Both structures are highly textured and make excellent successive approximations to a general polycrystalline material.

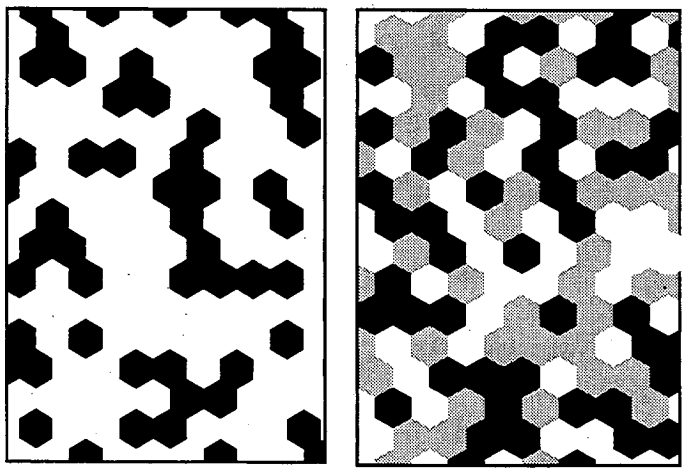

Figure 8: Schematic illustration of mazed bicrystal (left) and mazed tricrystal (right) microstructure as synthesized by thin film deposition of Al on Si single crystals.

A bright field image of a typical bicrystal film as produced by thin film deposition is shown in figure 9. One grain orientation is in Bragg condition and appears dark. Note the mazed intertwining faceted topography [13]

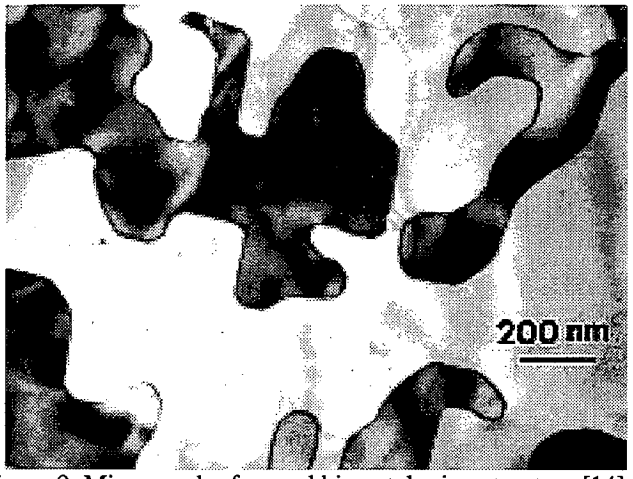

Figure 9: Micrograph of mazed bicrystal microstructure [14].

A composite diffraction pattern of the two variants is shown in figure 10 with one of the two patterns marked by black dots. The white lines indicate traces of mirror planes. Vertical and horizontal mirrors exchange the black and white variants and are thus color symmetry elements. Diagonal mirrors change each variant into itself and are thus grey mirrors.

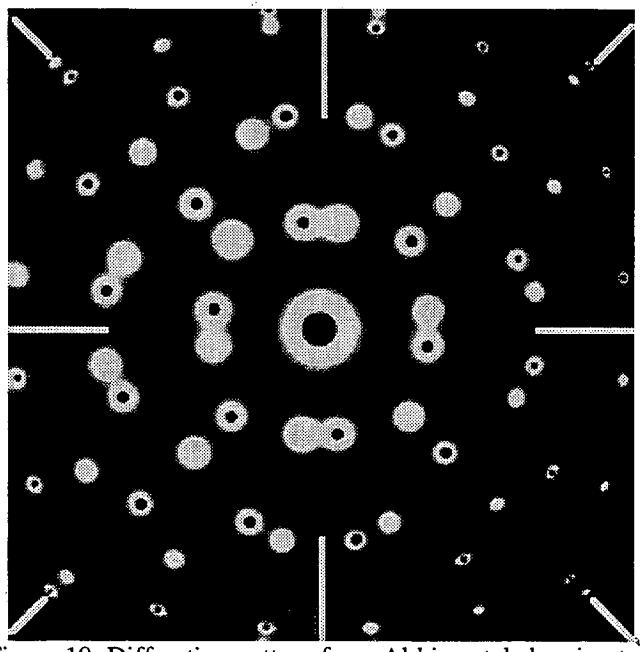
Figure 10: Diffraction pattern from Al bicrystal showing two <110> zone axis patterns rotated 90° relative to each other. For simplicity, one variant is marked with black dots. Symmetry elements are indicated by white lines.

A tricrystal film is shown in three complementary dark field images in figure 11. The tracing in (d) shows that the three orientation variants account for almost the entire film. It is also apparent that triple junctions are now frequently observed. This microstructure for the first time will allow study of the atomic structure of triple grain boundary junctions by high resolution electron microscopy [15,16].

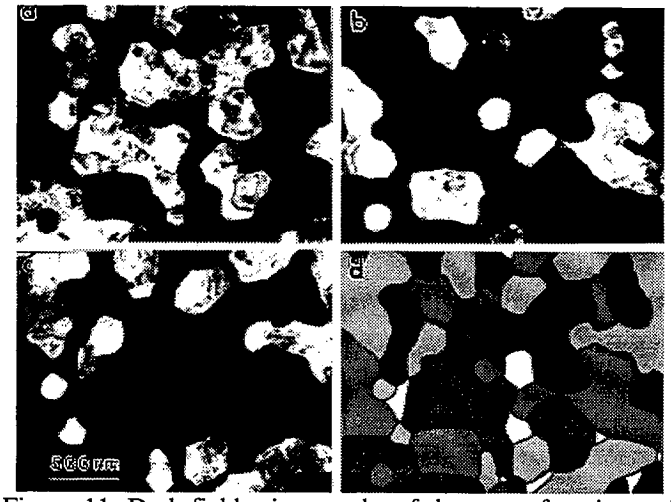

Figure 11: Dark field micrographs of the area of a tricrystal thin film, taken with reflections from three different orientation variants (a-c), and tracing of all three (d).

For comparison with the bicrystal, a composite tricrystal diffraction pattern is shown in figure 12. This pattern is made up of three <100> zone axis patterns of Al rotated 120° relative to each other. The resulting symmetry, ignoring variants, is 12-fold, with traces of mirror planes indicated. Thus, interestingly the composite symmetry of this microstructure is higher than that of the components.

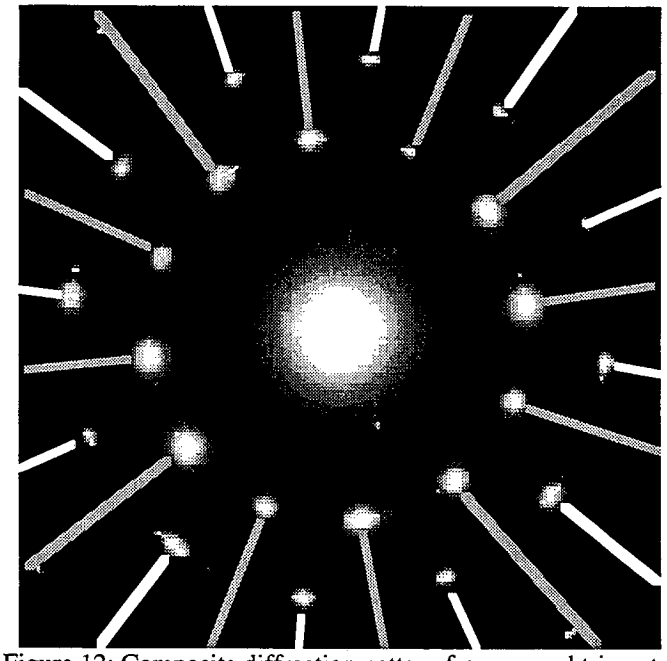
Figure 12: Composite diffraction pattern from mazed tricrystal thin film of Al formed by deposition on {111} Si substrate. The pattern is composed of three <001> orientations of Al, rotated 120° relative to each other and exhibits non-crystallographic 12mm symmetry.

III. SUMMARY

It has been shown that symmetry and broken symmetry plays an important role in the development of microstructures,

the analysis of their origins, texture, morphology and topography. Electron microscopy is an excellent tool for the detection and analysis of symmetry and its absence. A global approach to microstructure and its symmetry allows the design and synthesis of novel microstructures with interesting and unusual properties.

IV. ACKNOWLEDGEMENTS

It is a pleasure to acknowledge the enjoyable collaboration with K.H. Westmacott on most of this research and the important contributions of N. Thangaraj to the work on mazed bi- and tricrystal structures. This work is supported by the Director, Office of Energy Research, Office of Basic Energy Sciences, Materials Sciences Division of the U.S. Department of Energy under Contract No. DE-ACO3-76SFOOO98.

V. REFERENCES

[1] Cahn, J.W. (1977) Acta Met. 25, 721

[2] Dahmen, U. (1980) Acta Met. 30,63

[3] A.G. Khachaturyan, Theory of Structural Transformation in Solids, J. Wiley & Sons, New York (1983)

[4] U. Dahmen, P. Ferguson and K.H. Westmacott, Acta Met. 32, 803 (1984)

[5] Gratias, D., Portier, R. and Fayard, M. (1979) Acta Cryst, A35, 885

[6] Dahmen, U. and Westmacott, K.H. (1986) MRS Proc. 62, 217

[7] J.W. Cahn and G. Kalonji, Proc. Conf. Solid-Solid Phase Trans., (1981), eds. H.I. Aaronson et al., p.3

[8] e.g. Y.I. Sirotin, M.P. Shaskolskaya, Fundamentals of Crystal Physics, MIR Publishers, Moscow, USSR (1982)

[9] U. Dahmen, Ultramicroscopy 30, 102 (1989)

[10] Witcomb, M.J., Dahmen, U. and Westmacott, K.H. (1988) Proc. EMSA, 764

[11] U. Dahmen and K.H. Westmacott, Scr. Met. 22,1673 (1988)

[12] U. Dahmen and K.H. Westmacott, MRS 229, 167 (1991)

[13] N. Thangaraj, J. Reyes-Gasga, K.H. Westmacott and U. Dahmen, MRS 221, 81 (1991)

[14] N. Thangaraj, K.H. Westmacott and U. Dahmen, Appl. Phys. Lett., 61, 37 (1992)

[15] N. Thangaraj and U. Dahmen, MRS Proc. 238, 171 (1992)

[16] N. Thangaraj, K.H. Westmacott and U. Dahmen, Appl. Phys. Lett., 61, 913 (1992)

LAWRENCE BERKELEY LABORATORY
UNIVERSITY OF CALIFORNIA
TECHNICAL INFORMATION DEPARTMENT
BERKELEY, CALIFORNIA 94720